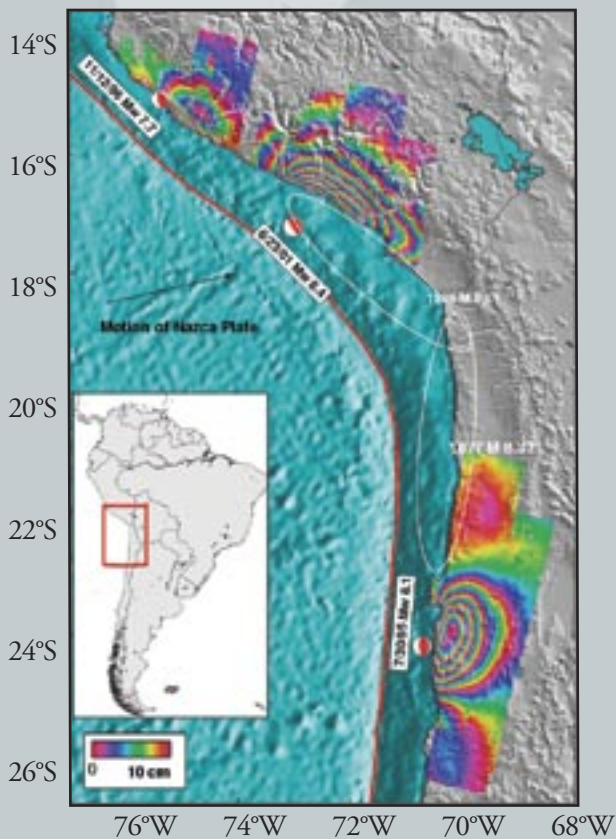


Using InSAR to Study Earthquakes in South America

by Matt Pritchard, Princeton University and Mark Simons, California Institute of Technology



The Nazca Plate is subducting eastward into the mantle below the western coast of South America at about 7 cm yr^{-1} . This collision causes high levels of volcanic activity and the long-term uplift of the Andes by compressional tectonics. On shorter timescales, this deformation manifests itself as large earthquakes along the entire length of the west coast of South America, including several earthquakes with magnitudes greater than 7.5 occurring in the past decade.

Earthquakes radiate seismic waves and cause permanent local crustal deformation that can be modeled to determine exactly which parts of a fault slipped (both at the surface and at depth) during that event. It is important to know which parts of a fault have slipped for many reasons. One common application of fault slip maps is to better characterize earthquake hazard. When one segment of a fault ruptures it can increase or decrease the stress on some of the neighboring segments of the fault, making an earthquake reoccurrence more or less likely in these regions.

In addition, if we know how the stress in the crust was modified by the earthquake, and can precisely measure how these stresses relax with time (by affecting surface deformation), we can constrain the mechanical properties of these regions. Using RADARSAT-1 and ERS radar data made available through ASF, we are combining InSAR observations with GPS measurements of deformation and seismographic recordings of the radiated seismic energy to construct fault slip maps.

The arid central Andes are an ideal location for InSAR, because the radar scattering properties of the ground change little between observations. Even though the InSAR observations are of high quality, it is not a straightforward matter to determine what parts of the fault slipped in these large earthquakes.

One particular problem with this area is that a large amount of fault slip occurs under water where, currently, no measurements of deformation can be made. Nonetheless, by combining the InSAR, GPS and seismic data, we can estimate the sites of fault slip and determine how these earthquakes might impact surrounding areas which may become the sites of future large earthquakes.

The image on this page shows the color contours of the satellite line-of-sight component of ground deformation from radar interferograms of three shallow thrust subduction zone earthquakes draped over shaded relief and bathymetry.

The white outlines enclose the approximate rupture areas of large earthquakes of the 19th century that will possibly re-rupture in the 21st century. Black lines show political borders, and the red line is the Peru-Chile trench. The region of interest is indicated in the reference map at the lower left. In the 1995, 1996 and 2001 earthquakes, South America moved to the west, but the events look slightly different because of the different locations of slip on the fault interface relative to the coastline and the size of each earthquake. Because the radar satellites measure primarily vertical deformation, we can interpret the gross features as portions of the ground that were uplifted or subsided.

Typically, for subduction zone earthquakes, we detect primarily subsidence on land, with uplift offshore. For the 1995 earthquake, a small region of dry land (the peninsula) was uplifted, and the closed contours in the interferogram are mostly caused by the on-land subsidence. For the 1996 earthquake, the slip was closer to land, so more uplift is recorded on-shore, but the closed contours represent subsidence. Most of the fault slip from the 2001 earthquake was off-shore, so only subsidence is measured on land. ♦

Building an Integrated View of Antarctica

by Kenneth C. Jezek, The Ohio State University

NASA and the Canadian Space Agency began planning in the early 1980s for an imaging campaign using Synthetic Aperture Radar to be carried by RADARSAT-1. The technical goals set forth in the early planning were to obtain two complete mappings of Antarctica. These would result in the first, high-resolution radar maps and provide nearly instantaneous snapshots of the icy continent.

The science driving the technical goal was to obtain benchmarks for detecting changes in the continent by comparison with earlier and subsequent data. Radar interferometry for ice sheet studies was proven with the European Earth Remote Sensing Satellite, but the Antarctic Mapping Mission (AMM) was the first dedicated use of RADARSAT-1 for radar interferometry for large-scale studies.

Preparing for the campaigns, organized under the RADARSAT-1 Antarctic Mapping Project (RAMP), took years of effort. The first AMM commenced in September 1997. During this phase, the primary mapping goal was achieved, capturing an extraordinary view of Antarctica that has been widely distributed to the science community in digital and hard-copy form.

The campaign also acquired 24-day, repeat-pass data suitable for interferometric analysis. Repeat-pass interferometry allows the computation of sub-wavelength scale estimates of surface displacement. Consequently, the surface velocity of the ice sheet can be calculated with such data from the ice divides to the ice margin.

The second campaign to image Antarctica began in September 2000 with a modified set of technical and scientific goals. Based on the quality of the AMM image map, there was great interest in securing a second map that could be used to measure changes in the coastal



*RADARSAT-1 SAR mosaic of Antarctica:
Light shading indicates strong backscatter;
and dark shading indicates weak backscatter.*

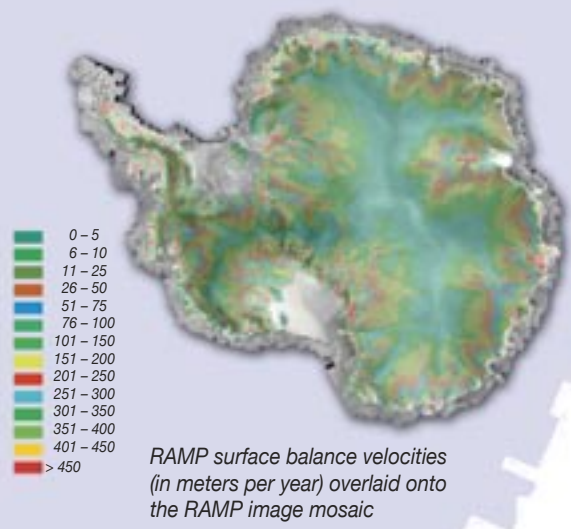
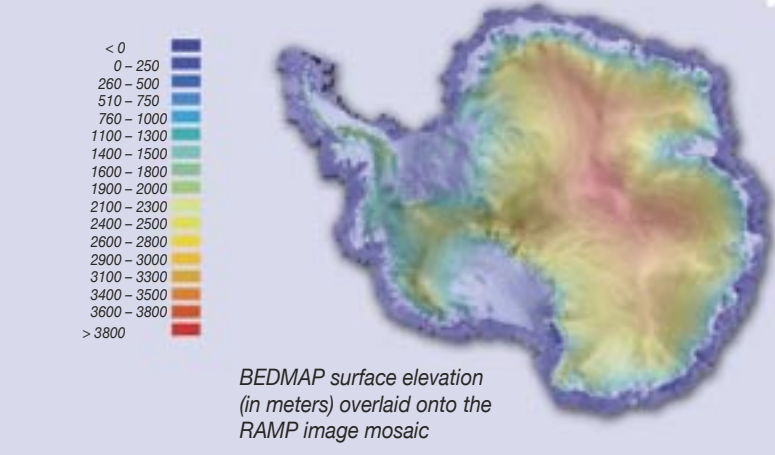
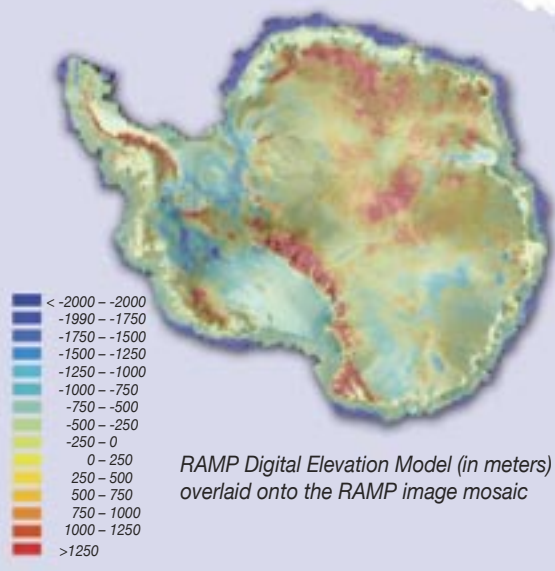
areas of Antarctica and changes in fast glaciers and ice streams. Because of the proven ability to acquire interferometric data, there was also great interest in using RADARSAT-1 to map as much of the surface velocity field as possible.

Three complete repeat mappings were acquired with each mapping containing complete ascending and descending data, the coverage extending from about 80 degrees south to the coast. The acquisition phase, known as the Modified Antarctic Mapping Mission (MAMM), was completed successfully. While the analysis of this large and complex data set is ongoing, the results are already proving to be of exceptional scientific interest.

The RAMP Antarctic image mosaic shown on this page was created using map attributes of high resolution and continental coverage. The mosaic has been used to: map the coastline of the continent in great detail; study and contrast glaciological regimes about the continent; and examine glaciological processes, such as the evolution of ice shelves, by observing ice shelves at various stages of development about the continent.

A single instrument or data set alone is rarely able to answer complex scientific questions, so it became useful and very interesting to use the RAMP mosaic as a basis for integrating other continental scale observations into a common framework referenced to features observable on the surface. We have assembled several continental data sets, including velocities computed from the MAMM data set, into a Geographic Information System format. In each case, the base map for the image is the AMM mosaic.

We examined surface topography patterns using the Digital Elevation Model developed as part of RAMP. The figure at the top right, on the next page, shows surface elevation expressed as colored tones overlaying the mosaic that governs the brightness. This image clearly shows the relationship between the ice divides which partition the ice sheet into different catchment basins and well defined tonal patterns in the SAR mosaic. The physical link between ice divide and backscatter remains unknown, but the obvious correlation provides



useful information on the detailed positions of ice divides.

We next compare the RAMP mosaic with the BEDMAP compiled, basal topography shown in the center of the figure on this page. Good correlations between the basal topography and backscatter strength are notable in the vicinity of the Belgica Highlands (lower right quadrant). These results are exciting, while not completely unexpected, since established theory relates basal topography, surface topography, and accumulation patterns.

The correlations found between basal topography and backscatter

strength suggest that inferences about basal topography and properties can be made using the image mosaic in regions where basal topography data are sparse or completely absent.

Surface velocity is a key, kinematic variable for estimating ice sheet mass balance and is a diagnostic indicator of the forces governing ice-sheet dynamics.

A comparison of the RAMP model of surface balance velocities and the mosaic is shown at the bottom on this page. Balance velocities are computed using information on accumulation rate, ice thickness and surface slope, under the assumption that the ice sheet is in mass balance. The velocity patterns capture the extensive network of ice streams draining into the Filchner Ice Shelf (upper left of center quadrant).

These ice streams are revealed in the RAMP mosaic by the intense crevassing that occurs along their margins and which appears bright in radar imagery.

The RAMP balance velocity model becomes more interesting when compared to measured velocities. Statistically significant differences can be attributed to places where the ice sheet is in fact either thickening or thinning. A comparison between the balance velocity model and MAMM interferometrically derived surface velocities reveals that the balance and measured velocities agree generally between the two, but what is especially interesting is the presence of numerous small ice streams or outlet glaciers revealed in the MAMM data and that snake through the area north of the Amery Ice Shelf.

Continental scale, high-resolution data sets of Antarctica are becoming available from a host of satellites carrying on board a suite of sensors that span the electromagnetic spectrum. New sensors are being planned or are already on the way that will greatly improve existing measurements, and some novel instruments are now being designed to acquire key geophysical observations of Antarctica's physical properties from space for the first time.

Continuing the acquisition and compilation of these data into the future will provide a crucial four-dimensional look at Antarctica, and indeed, our entire home planet. We need such a look to understand how our planet is changing and what role we play in that change.

Acknowledgements: The RADARSAT Antarctica Mapping Project is a collaboration between the Canadian Space Agency and NASA. Processing and analysis of the RAMP data is supported by a grant from NASA's Pathfinder Program and Polar Oceans and Ice Sheets Program. RAMP participants include the Jet Propulsion Laboratory, the Alaska Satellite Facility, Vexcel Corporation and The Ohio State University. ♦

Studying Aleutian Volcanoes With InSAR

Satellite InSAR has proven a powerful spaceborne geodetic tool to study varied volcanic processes by analyzing surface deformation patterns. With the implementation of InSAR technology, volcano monitoring has entered an exciting phase wherein magma accumulation in the middle to upper crust can be observed long before the onset of short-term eruption precursors.

Ultimately, more widespread use of InSAR for volcano monitoring could shed light on a part of the eruption cycle—the time period between eruptions when a volcano seems to be doing essentially nothing. Combining InSAR technique with observations from continuous GPS, gravity, strainmeters, tiltmeters, seismometers and volcanic gas studies will improve our capability to forecast future eruptions and lead to improved volcano hazard assessments and better eruption preparedness.

Kiska Volcano

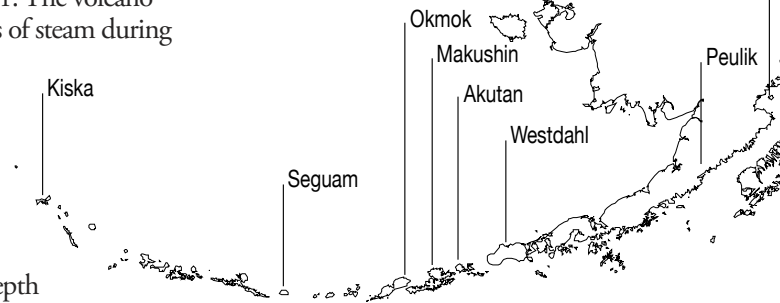
Kiska volcano is the westernmost historically active volcano in the Aleutian arc. InSAR images of Kiska show a circular area about 3 km in diameter centered near the summit subsided by as much as 10 cm from 1995 to 2001. The volcano emitted copious amounts of steam during recent eruptions. Field reports document vigorous steaming and persistent ground shaking near the summit. Based on these reports and the shallow source depth (<1 km), the observed subsidence is attributed to decreased pore-fluid pressure within a shallow hydrothermal system beneath the summit area.

Seguam Volcano

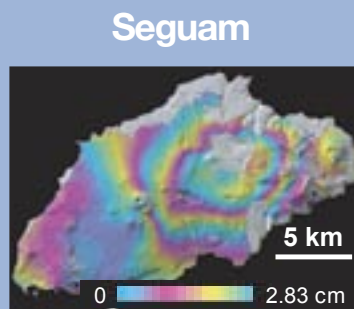
Seguam volcano, often referred to as Pyre Peak, erupted in 1901, 1927, 1977 and 1992-93. InSAR images, spanning various intervals during 1992-2000, document co-eruptive and post-eruptive deformation of the 1992-93 eruption. A model that combines magma influx, thermoelastic relaxation, and poroelastic effects accounts for the observed deformation. This example demonstrates that spatial and temporal coverage with InSAR data reveals dynamic processes within a volcano.

Okmok Volcano

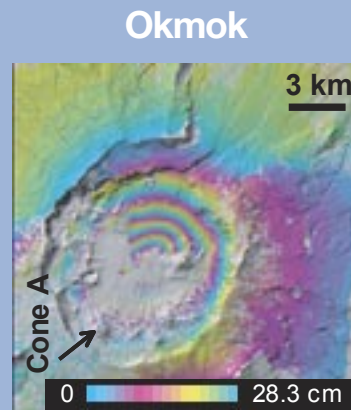
Okmok volcano, a broad shield topped with a 10-km-wide caldera, produced blocky basaltic flows during relatively large effusive eruptions in 1945, 1958 and 1997. Multiple InSAR images mapped: 1) the surface inflation of more than 18 cm during 1992-95 and subsidence of 1-2 cm during 1995-96, prior to the 1997 eruption; 2) more than 140 cm of surface deflation during the 1997 eruption; and 3) 5-15 cm/year inflation during 1997-2003, after the 1997 eruption. Numerical modeling suggested the magma reservoir responsible for the observed deformation resided at a depth



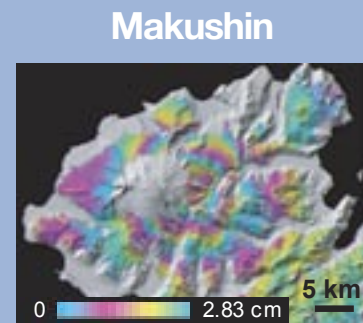
The interferogram for Kiska volcano above shows subsidence of the volcano summit during August 1999 and August 2000. This and other interferograms in this report are draped over the DEM shaded relief images and areas without interferometric coherence are uncolored.



The interferogram of Seguam volcano above shows uplift of the island from July 1999 to September 2000.



The interferogram (October 1995 – September 1997) above, bracketing the February – April 1997 eruption, shows the volcano deflated more than 1.4 m due to magma withdrawal. The location of the 1997 vent is labeled Cone A.



The interferogram of Makushin volcano above shows about 7 cm of inflation associated with a possible eruption in January 1995.

by Zhong Lu, USGS, EROS Data Center, SAIC; Chuck Wicks, USGS, Earthquake & Volcano Hazards Programs; Dan Dzurisin, USGS, Cascades Volcano Observatory; John Power, USGS, Alaska Volcano Observatory



of about 3 km beneath the center of the caldera and about 5 km away from the eruptive vent. This example demonstrates how InSAR is capable of measuring pre-eruptive, co-eruptive, and post-eruptive deformation in the subarctic environment.

Makushin Volcano

Makushin volcano, a broad, ice-capped, truncated stratovolcano, is one of the more active volcanoes in the Aleutians, producing at least 17 explosive, relatively small eruptions since the late 1700s. Additional smaller eruptions probably occurred during this period but were unrecorded, either because they occurred when the volcano was obscured by clouds or because the eruptive products did not extend beyond the volcano's flanks.

Several independent InSAR images that each span the time period from October 1993 to September 1995 show evidence of ~7 cm of uplift centered on the volcano's east flank. The uplift was interpreted as pre-eruptive inflation of a small explosive, but unsubstantially reported, eruption on January 30, 1995. This example demonstrates that ground deformation of a few cm can be unambiguously identified with InSAR images over a rugged terrain where geometric distortion of radar images is severe.

Akutan Volcano

Akutan, the second most active volcano in Alaska, was shaken in 1996 by an intense earthquake swarm accompanied by extensive ground cracking, but no eruption of the volcano. Both L-band JERS-1 and C-band ERS-1/2 InSAR images show uplift of as much as 60 cm on the western part of the island associated with the swarm. Our JERS-1 interferogram, displaying greater coherence, especially in areas with loose surface material or thick vegetation, also shows subsidence of similar magnitude on the eastern part of the island, and displacements along faults reactivated during the swarm.

The axis of uplift and subsidence strikes about N70°W and is roughly parallel to: 1) a zone of fresh cracks on the volcano's northwest flank, 2) normal faults that cut the island, and 3) the inferred maximum

compressive stress direction. Both before and after the swarm, the northwest flank uplifted 5-20 mm/year relative to the southwest flank, probably by magma intrusion. This example demonstrates that InSAR can provide a basis not only for interpreting and modeling movement of shallow magma bodies that feed eruptions, but also for detecting intrusive activities that do not result in an eruption.

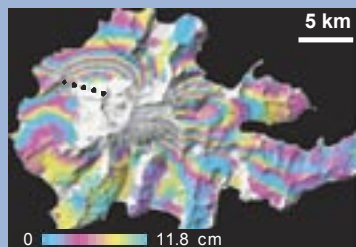
Westdahl Volcano

Westdahl volcano, a young glacier-clad shield volcano had documented eruptions in 1964, 1978-79 and 1991-92. The background level of seismic activity since the last eruption has been generally low (about five $M < 3$ earthquakes per year). InSAR images during 1991-2000 show that Westdahl volcano deflated during its 1991-92 eruption and is re-inflating at a rate that could produce another eruption in the next several years.

The rates of post-eruptive inflation and co-eruptive deflation are approximated by exponential decay functions with time constants of about 6 years and a few days, respectively. This behavior is consistent with a deep, constant-pressure magma source connected to a shallow reservoir by a magma-filled conduit where the magma flow rate is governed by the pressure gradient between the deep source and the shallow reservoir.

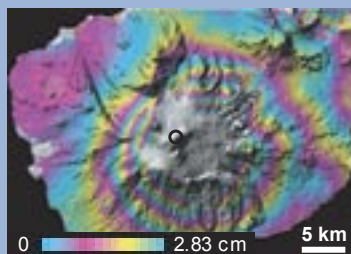
Continued on page 6

Akutan



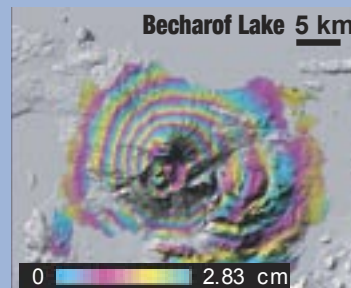
The interferogram of Akutan volcano above, spanning the March 1996 seismic swarm, shows uplift of more than 60 cm on the western part of the island and subsidence of similar magnitude on the eastern part of the island. The dashed line represents a zone of ground cracks created during that activity.

Westdahl



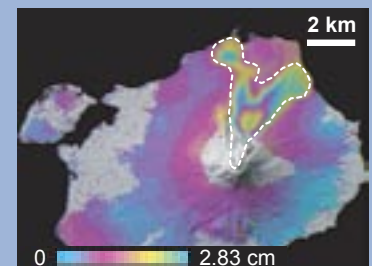
Aseismic inflation of Westdahl volcano, observed from a 1993-98 InSAR image, is shown above with a circle representing the horizontal position of the shallow magma reservoir beneath the peak.

Peulik



The interferogram (October 1996 - October 1997) above indicates about 17 cm of uplift of Peulik volcano. The aseismic inflation occurred before the May 1998 earthquake swarm near Becharof lake, about 30 km northwest of the volcano.

Augustine



The interferogram (1992-1993) of Augustine volcano above depicts the deformation associated with the compaction of the 1986 pyroclastic flow deposits outlined by the white dashed line.

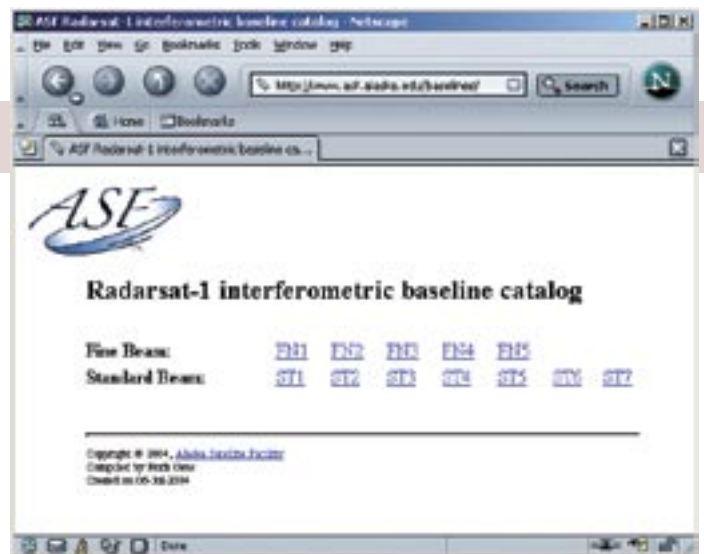
The ASF RADARSAT-1 Interferometric Baseline Catalog

Increased use of RADARSAT-1 fine beam and standard beam data for interferometric projects has intensified the growing demand for baseline information corresponding to data acquired over numerous regions of interest to researchers. ASF has recently developed an interferometric baseline catalog for RADARSAT-1 data using metadata contained in the scan results file, generated when the raw telemetry signal is captured to a digital file.

Baseline information for the new catalog is estimated on an ASF frame basis using state vectors, the Doppler centroid and the slant range. The baselines for existing image pairs in the ASF archive up to RADARSAT-1 orbit 45000 are now stored in a database that serves as the backbone of a web interface found at <http://www.asf.alaska.edu/baselines/>.

The archive at ASF contains some 2-million suitable image pairs for interferometric use. Orbits containing interferometric frames are separated in the baseline catalog by beam mode, fine and standard beam, and are organized by month and year of acquisition.

Further details about the development of the catalog at ASF are described in the paper *Development of a RADARSAT-1 Interferometric Baseline Catalog* presented by Rudi Gens at the IGARSS 2004 conference in Anchorage, Alaska. ♦



The Web interface for the baseline catalog is shown above; below is a table reflecting the distribution of data with respect to beam mode.

	Repeat Orbits	InSAR Frames
FN1	1325	65242
FN2	220	8307
FN3	120	2696
FN4	175	5501
FN5	82	2291
ST1	3228	323581
ST2	4094	445600
ST3	2510	331834
ST4	1918	202047
ST5	2006	223103
ST6	2975	272687
ST7	2186	208446

Studying Aleutian Volcanoes With InSAR *continued*

This example demonstrates that:
 1) InSAR is becoming the best tool available for detecting deep, aseismic magma accumulation by measuring broad, subtle deformation of the ground surface to identify restless volcanoes long before they become active and before seismic and other precursors emerge and 2) multi-temporal InSAR images enable construction of a virtual magma plumbing system that can be used to constrain magma accumulation at the shallow reservoir and shed light on the time window of the next eruption.

Peulik Volcano

Peulik volcano, a stratovolcano located on the Alaska Peninsula, is known to have erupted in 1814 and 1852. InSAR images that collectively span the time interval from July 1992 to August 2000 reveal that a presumed magma body

located 6.6 km beneath the Peulik volcano inflated 0.051 km³ between October 1996 and September 1998.

The average inflation rate of the magma body was about 0.003 km³/month from October 1996 to September 1997; peaked at 0.005 km³/month from June 26 to October 9, 1997; and dropped to 0.001 km³/month from October 1997 to September 1998. Deformation before October 1996 or after September 1998 is not significant. An intense earthquake swarm occurred about 30-km northwest of Peulik from May to October 1998, around the end of the inflation period.

The 1996-98 inflation episode at Peulik confirms that InSAR can be used to detect magma accumulation beneath dormant volcanoes at least several months before other signs of unrest are apparent. This application represents a first step toward understanding the eruption cycle

at Peulik and other stratovolcanoes with characteristically long repose periods.

Augustine Volcano

Augustine volcano, an 8-by-11 km island, has had six significant eruptions in the last two centuries: 1812, 1883, 1935, 1963-64, 1976, and 1986.

InSAR images show the pyroclastic flows from the 1986 eruption have been experiencing subsidence/compaction at a rate of about 3 cm/year, and no sign of significant volcano-wide deformation was observed during 1992-2000. The observed deformation can be used to study the characteristics of the pyroclastic flows.

For more information about this volcano monitoring project, please visit http://edc.usgs.gov/Geo_Apps or contact lu@usgs.gov. ♦

Mapping Glacier Velocity in Greenland

by Eric Rignot, Jet Propulsion Laboratory

The Greenland Ice Sheet is a vast expanse of ice which accumulates mass in the interior from snowfall and flows slowly toward the ocean where it is discharged along narrow channels occupied by outlet glaciers and ice streams.

Until a decade ago, we did not know whether the ice sheet was gaining or losing mass in response to climate change. In the 1990s, the NASA Polar Program initiated a research plan to determine the mass balance of the ice sheet using a combination of satellite data, airborne surveys, and in-situ measurements. The results show that the ice sheet is overall in balance in the interior regions, but is losing mass along the coast, and that overall it is contributing to a rise in sea level. Synthetic aperture radar interferometry (InSAR) is one of the techniques employed to study the ice sheet. With ERS-1 and ERS-2 SAR data from ASF, we demonstrated that InSAR can map ice velocity and topography at an unprecedented level of spatial detail and accuracy. We also found that InSAR can detect the transition boundary between grounded ice and floating ice, and it can detect changes in flow speed with time.

Our results yielded a detailed view of the discharge coming from the northern and eastern sectors of the ice sheet and the discovery of ice streams reaching far inland. InSAR revealed that in the northern part of Greenland, glaciers were melting

more from the bottom, as they reached the ocean, than from the top, and iceberg production was comparatively small. InSAR estimates of mass balance also showed that the north was slowly thinning, the east coast was close to balance but thinning, and the southeastern coast was largely out of balance and rapidly thinning.

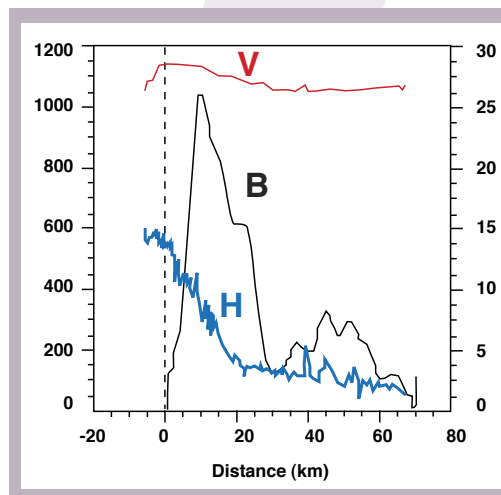
Then in 2001, a team of researchers initiated a detailed study focusing on the melt regime of the floating tongue of the Petermann Glacier, a major glacier in northwestern Greenland. This project is funded by NASA's Cryospheric Science Program and NSF's Arctic Research Program. The study involved detailed airborne surveys of the tongue, ground penetrating radar surveys, GPS surveys, automated weather stations, phase sensitive radar surveys, ablation measurements, and more recently, ice drilling.

The InSAR figure on this page shows a velocity map of Petermann Glacier that was derived from RADARSAT-1 data acquired in fall 2000. This velocity map was combined with a map of ice thickness from NASA/University of Kansas' ice sounding radar to calculate the glacier flux and its changes along flow. Those changes map directly into the bottom melting regime of the ice tongue. The

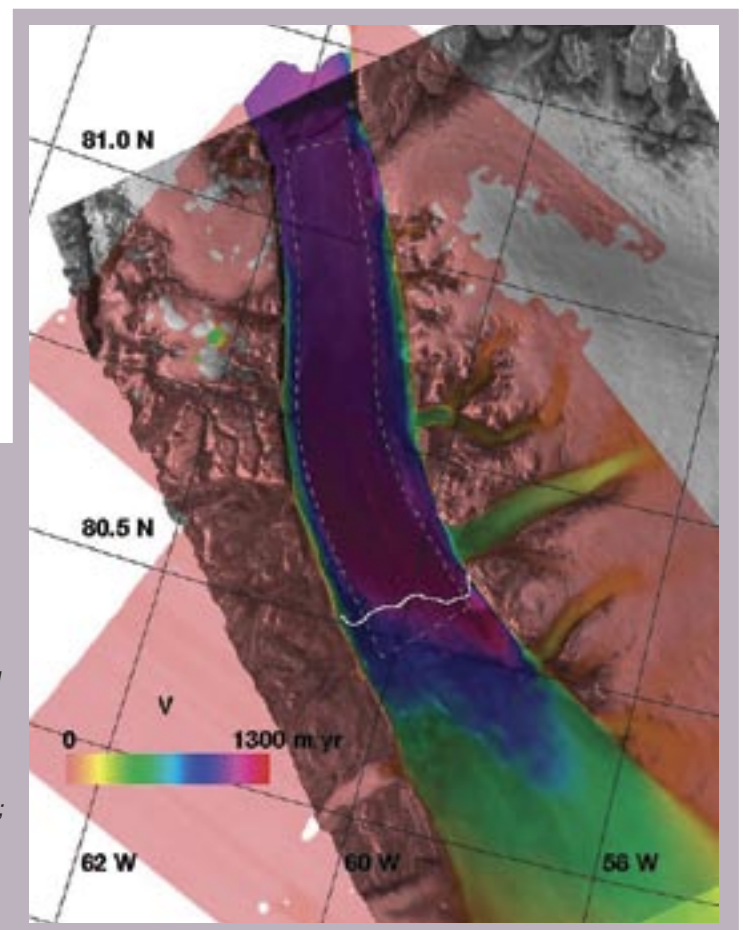
bottom melt rates reach 25 m/yr close to the grounding line, so that half of the glacier ice is removed from the bottom by the time the glacier advances 10 km, in 10 years. In a more detailed analysis of the SAR signal, we have also shown that bottom melting is strongly channelized, with sub-glacial river channels slowly eroding the ice shelf.

Near the ice front, the floating tongue of Petermann Glacier is only a few meters above the ocean surface. An increase in summer melt from warmer air temperatures, or in bottom melt from a warmer ocean, will have a major impact on the survival of the floating ice shelf, and in turn on the land ice discharge from this sector of the Greenland Ice Sheet into the Arctic ocean.

We are now collecting RADARSAT-1 data over Petermann Glacier on a regular basis, with the help of ASF and the Canadian Space Agency, to monitor the delicate equilibrium of melt/accumulation/ice flow processes on the floating tongue in a warming climate. ♦



The Petermann Glacier velocity map is shown at the right with a solid white line for the grounding line and a dotted white line showing the area where bottom melting was calculated. In the graph at the left, B is the bottom melting rate in m/yr, scaled down the right; while V is velocity in m/yr and H is ice thickness in m, both scaled down the left.



InSAR Workshop Advocates Community Participation

A community-led InSAR Working Group dedicated to the advancement of radar remote sensing research was established by the scientific community. The working group held a 3-day workshop October 20-23, 2004, to define science objectives that can be addressed through the use of InSAR, technology options, mission architecture scenarios and ideas for community education. Some 220 scientists participated in the event. The meeting resulted in documents outlining the science drivers, targets, and requirements

for an InSAR mission, and an outline of future participation in community advocacy for radar science. Intense interest in crustal deformation science related to earthquakes, volcanoes, and hydrologic processes, Earth surface-related global change such as the deformation of ice sheets and glaciers, and natural disaster response technology leads the U.S. scientific community to a strong advocacy for acquiring one or more dedicated InSAR-capable satellites in support of this research. An InSAR mission would greatly advance our understanding of basic processes affecting life on Earth. Only community involvement and backing of a U.S. InSAR mission will make such a satellite a reality.

ASF is pleased to name Scott Arko as the new Deputy Director. A three-and-a-half year ASF staff member, as both Engineering Center Manager and Lead Developer, Scott was responsible for managing many of the system upgrades at ASF.

Scott's formal education is in physics. He has a B.A. from Lawrence University in Wisconsin and an M.S. degree from Colorado State University. Before coming to ASF, Scott worked in the defense industry for 7 years. Working for the Ballistic Missile Defense Agency, Air Force Research Laboratory and Veridian Systems, he was involved in new technology development for the next generation of DoD airborne and spaceborne systems.

Alaska Satellite Facility
UAF Geophysical Institute
903 Koyukuk Drive
PO Box 757320
Fairbanks, AK 99775-7320



www.asf.alaska.edu



Submissions and Subscriptions

This newsletter, published by the Alaska Satellite Facility, was created to provide detailed information about special projects and noteworthy developments, as well as science articles highlighting the use of ASF data.

To receive the newsletter by postal mail, please fill out the subscription form linked to the ASF homepage at www.asf.alaska.edu. Current and back issues of the newsletter can also be obtained in PDF format through the ASF website.

Submissions to the *News & Notes* and suggestions about content are always welcome. If you are interested in contributing materials, please call or send an email to the editor:

Cheryl Katje, ASF User Services
907-474-6166
uso@asf.alaska.edu

Alaska Satellite Facility Office of the Director

Nettie La Belle-Hamer Director
Scott Arko..... Deputy Director

ASF Center Managers

Scott Arko(Acting) Engineering
Don Atwood..... Remote Sensing Support
Carel Lane..... Operations